RESEARCH ARTICLE

Figures and figure supplements

Mitochondrial MICOS complex genes, implicated in hypoplastic left heart syndrome, maintain cardiac contractility and actomyosin integrity

Katja Birker, Shuchao Ge and Natalie J Kirkland *et al*.

A

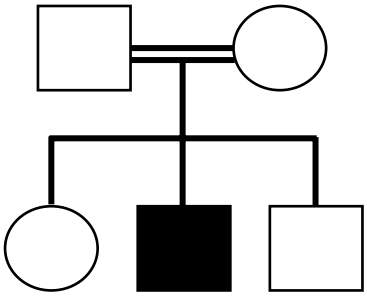

B

Human Gene	Fly Gene	DIOPT	Fly phenotype when knocked down (*Hand*$^{4.2}$)
RHBDL2	*rho-4*	6	none
CAP1	*capt*	14	Constricted, ↓ Cardiac output
SZT2	No fly ortholog		
RNF149	*gol*	7	none
CHCHD6	*Chchd3/6*	6	↓↓ Contractility
MTRR	*CG14882*	8	none
MBTPS1	*S1P*	14	none
DGKE	*Dgkepsilon*	13	Arrhythmic, Dilated
C17orf67	No fly ortholog		

C

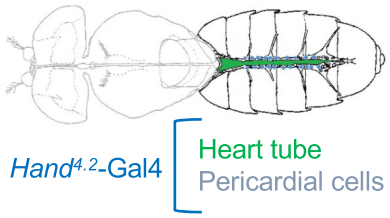

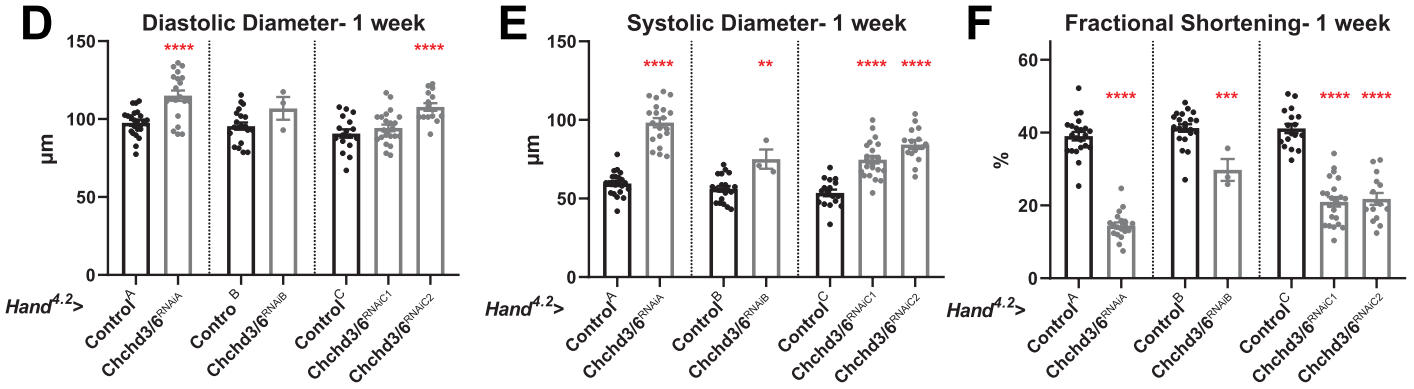

Figure 1. Prioritization of *CHCHD6* in HLHS proband and its *Drosophila* ortholog *Chchd3/6*. (**A**) Pedigree of index family 11 H. The family includes consanguineous parents (denoted by double horizontal lines) without cardiac defects, one son with HLHS (proband), and two siblings without cardiac defects. (**B**) List of 9 candidate genes derived from proband 11 H with corresponding *Drosophila* orthologs. Orthology based on DIOPT score. Conserved *Drosophila* candidate HLHS genes were knocked down individually in the *Drosophila* heart using the *Hand*$^{4.2}$*-Gal4* driver. The functional phenotypes listed were significantly different relative to Control^{A} or Control^{B} and were measured in 1 week old female *Drosophila* hearts. (**C**) Schematic of *Drosophila* highlighting the abdominal region which includes the heart tube and flanking pericardial cells, where the *Hand*$^{4.2}$-Gal4 driver is expressed. Image adapted from Figure 1A of ***Xie et al., 2013***. (**D**) End-Diastolic diameter (EDD), (**E**) End-systolic diameter (ESD), and (**F**) fractional shortening (FS) from 1 week old female *Hand*$^{4.2}$*-Gal4>Chchd3/6* flies.

Figure 1—figure supplement 1. *Chchd3/6* KD in the *Drosophila* heart causes reduced fractional shortening due to systolic dysfunction. (**A**) EDD, (**B**) ESD and (**C**) FS from 3 week old *Hand*$^{4.2}$>*Chchd3/6* female flies. Very low number of *Hand*$^{4.2}$>Chchd3/6^{RNAiB} flies reaching 3 weeks-of-age indicates lethality possibly due to stronger KD of *Chchd3/6*. (**D–F**) 1 week old *Hand*$^{4.2}$-*Gal4*, tdtK >*Chchd3/6* female flies measured for (**D**) EDD, (**E**) ESD and (**F**) FS. (**G**) Confocal images of *Chchd3/6* mRNA and *tinman* mRNA inside adult cardiomyocytes (top; nuclei are outlined) and processed images (bottom). (**H–I**) *Chchd3/6* and *tinman* mRNA in 1 week old female *Drosophila* hearts. (**H**) *Chchd3/6* mRNA relative to *tinman* mRNA is reduced in *Hand*$^{4.2}$>Chchd3/6^{RNAiA} heart tissue. (**I**) *tinman* mRNA % area, used as marker to normalize expression to. Fractional shortening in control and *Chchd3/6* KD female flies at 3 weeks of age with a (**J**) pericardial cell-specific driver (*DOT*-Gal4), (**K**) all muscle cell specific driver (*Mef2*-Gal4), and (**L**) neuronal driver (*elav*-Gal4).

Figure 1—figure supplement 1 continued on next page

Figure 1—figure supplement 1 continued

Note that *Mef2* >*Chchd3/6*^{RNAiA} was lethal at pupal stages. (**M**) Fractional shortening measurements from *Hand*$^{4.2}$>Duox^{RNAiC} 3-week-old flies. Unpaired two-tailed t-test, *P≤0.05, **P≤0.01, ***P≤0.001, ****P≤0.0001; error bars represent SEM.

Figure 2. *Chchd3/6* expression is important for adult cardiac function around larval stages and early adult stages. (**A**) UMAP (uniform manifold approximation and projection) plot from CB-specific single-cell transcriptomics (***Vogler, 2021a***) showing expression of *Chchd3/6* in CBs, as identified by cardiac TFs *tin*, *H15*, and *Hand*. (**B**) Stage 16–17 embryos (late stage cardiogenesis) were collected from a *Chchd3/6* loss of function line (*Chchd*^{D1}) line crossed to a *Chchd3/6* deficiency line (*Chchd*^{DefA}) and stained for Mef2 (all muscle transcription factor, magenta) and Slit (secreted protein of

Figure 2 continued on next page

Figure 2 continued

the lumen, green). 50 μm scale. (**C**) *tinD* >Control^{A} or>Chchd3/6^{RNAiA} were reared at 29 °C and females were filmed and imaged at 1 week of age. (**A**) *tinD* >Chchd3/6^{RNAiA} did not have a significant reduction in fractional shortening compared to *tinD* >Control^{A} flies. (**D**) F-actin was unchanged between *tinD* >Control^{A} and *tinD* >Chchd3/6^{RNAiA} flies at 1 week of age; 20 μm scale. (**E**) Schematic overview of temperature shift experiments. (**F–I**) Fractional shortening measurements from 1 week old female flies reared at (**F**) 19 °C for whole life, (**G**) at 29 °C for whole life, (**H**) 19 °C, and moved to 29 °C at early pupal stages, or (**I**) 19 °C, and moved to 29 °C once eclosed (virgin flies), Unpaired two-tailed t-test, ****$P \leq 0.0001$, error bars represent SEM.

Figure 3. Cardiac tissue from heart-specific *Chchd3/6* KD flies exhibit reduced and altered sarcomeric proteins in the myocardial tissue. (**A**) Schematic of sarcomeric protein distribution inside myofibrils (image created with BioRender.com). (**B**) F-actin staining in 1 week old female *Drosophila* hearts with *Hand*$^{4.2}$-*Gal4* KD of *Chchd3/6*. Arrowheads indicate ostial myofibrils and arrows point to myocardial myofibrils (non-ostial). (**C**) F-actin intensity measured as mean gray value (gray value/# of pixels) along myocardial myofibrils relative to mean gray value of ostial myofibrils. (**D**) Mean intensity of F-actin along

Figure 3 continued on next page

Figure 3 continued

individual myofibrils. 1 week old *Drosophila* hearts with *Hand*$^{4.2}$-*Gal4* driven KD of control or *Chchd3/6* stained for antibodies against (**E**) Myosin, (**F**) Obscurin, (**G**) α-Actinin, or (**H**) Sallimus. Arrowheads indicate ostial myofibrils and arrows point to working cardiomyocyte tissue (non-ostial). (**I–L**) Mean fluorescence intensity along myocardial myofibrils relative to ostia myofibrils in 1 week old *Hand*$^{4.2}$-*Gal4*>CHCHD3/6^{RNAiA} adults stained for sarcomeric proteins (**I**) Myosin, (**J**) Obscurin, (**K**) α-Actinin, or (**L**) Sallimus. Unpaired two-tailed t-test, $^{**}P \leq 0.01$, $^{****}P \leq 0.0001$; error bars represent SEM. 20 μm scale.

A

Human	Fly	Phenotype (Hand$^{4.2}$; tdtK>)
Cofilin	tsr	lethal
		lethal
Profilin	chic	none
		lethal
Arp2/3	Arp	↓ FS (↑ SD), moderate myofibrillar disorganization
		none
Gelsolin	gel	↓ FS (↑ SD)
		none
Transgelin	Chd64	none
		↓ FS (↓ DD), moderate myofibrillar disorganization
WASP	WASp	↓ FS (↓ DD), strong myofibrillar disorganization
		↓ FS (↓ DD)
WIP	Verprolin 1	none
		none
Formins	DAAM	none
		none
Tropomyosin	Tm1	↓ FS (↑ SD)
		none

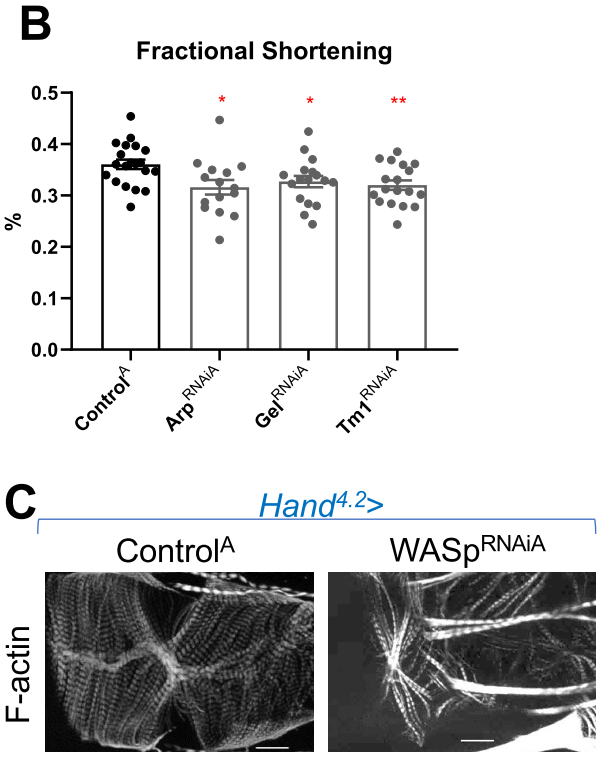

Figure 3—figure supplement 1. (**A-C**) Candidate genes involved in polymerization/de-polymerization of F-actin phenotypes upon KD using a *Hand*$^{4.2}$-Gal4;tdtK^{attP2} driver, measured at 1 week of age. (**B**) Fractional shortening from RNAi^{A} lines. (**C**) F-actin phenotype of hits. 20 µm scale. Unpaired two-tailed t-test, *$P \leq 0.05$, **$P \leq 0.01$; error bars represent SEM. FS = fractional shortening, DD = End diastolic diameter, SD = Systolic diameter.

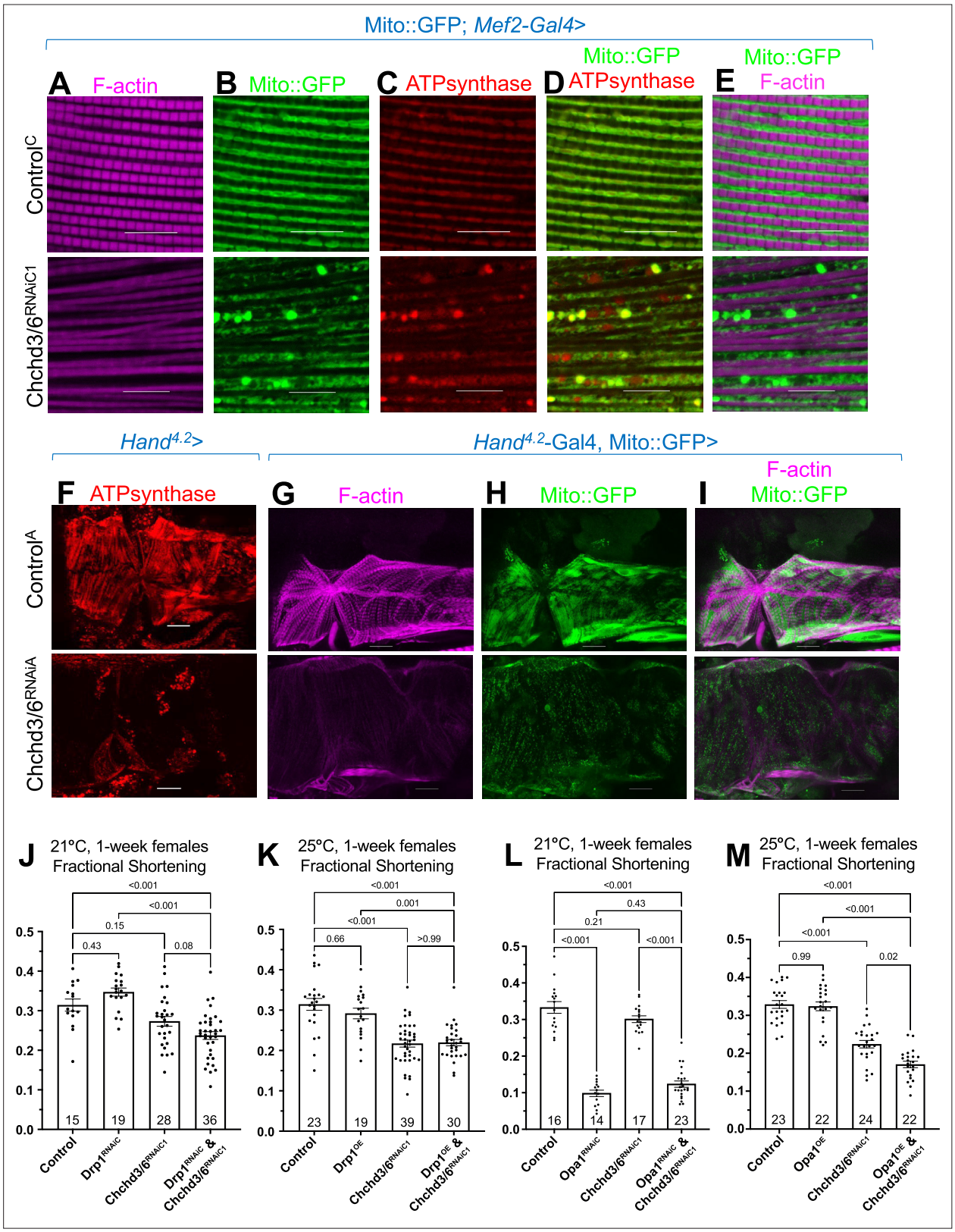

Figure 4. Mitochondrial fission-fusion defects were observed in cardiac *Chchd3/6* KD. (**A–E**) Visualization of F-actin and mitochondria in *Drosophila* indirect flight muscles (IFMs). 1–2 day-old male *Drosophila* IFMs with Mito::GFP; *Mef2*-Gal4 stained for (**A**) F-actin, (**B**) GFP (Mito::GFP (GFP tagged COX8A)), (**C**) ATP synthase, (**D**) merged image of B+C, and (**E**) merged image of A+B,10μm scale. (**F**) *Hand*$^{4.2}$>Chchd3/6^{RNAiA} heart tissue at 1 week of age. (**G–I**) F-actin and Mito::GFP staining in 1 week old female hearts using the *Hand*$^{4.2}$-*Gal4*; Mito::GFP driver, 20 μm scale. (**J–M**) Fractional shortening

Figure 4 continued on next page

Figure 4 continued

results are displayed from 1 week old females with manipulation of mitochondrial fission-fusion genes and *Chchd3/6*^{RNAiC1}. (**J**) *Chchd3/6* and *Drp1* KD at 21 °C had little effect on their own, but in combination caused a reduction in fractional shortening, displaying a significant genetic interaction (***Figure 3—figure supplement 1C***). (**K**) At 25 °C *Chchd3/6* KD reduced fractional shortening substantially, whereas *Drp1* OE by itself or in combination with *Chchd3/6*^{RNAiC1} had no effect, thus no genetic interaction was observed (***Figure 3—figure supplement 1F***). (**L**) Even at 21 °C, *Opa1* KD drastically reduced contractility, which in combination with *Chchd3/6* KD slightly improved, which resulted in a significant genetic interaction (***Figure 3—figure supplement 1I***). (**M**) At 25 °C, *Opa1* OE (**M**) had no effect, but in combination with *Chchd3/6* KD contractility was further reduced significantly, although the interaction p-value did not reach significance (***Figure 3—figure supplement 1L***). One-way ANOVA with multiple comparisons shows mean with SEM and associated p-values. Sample size is shown at bottom of each bar.

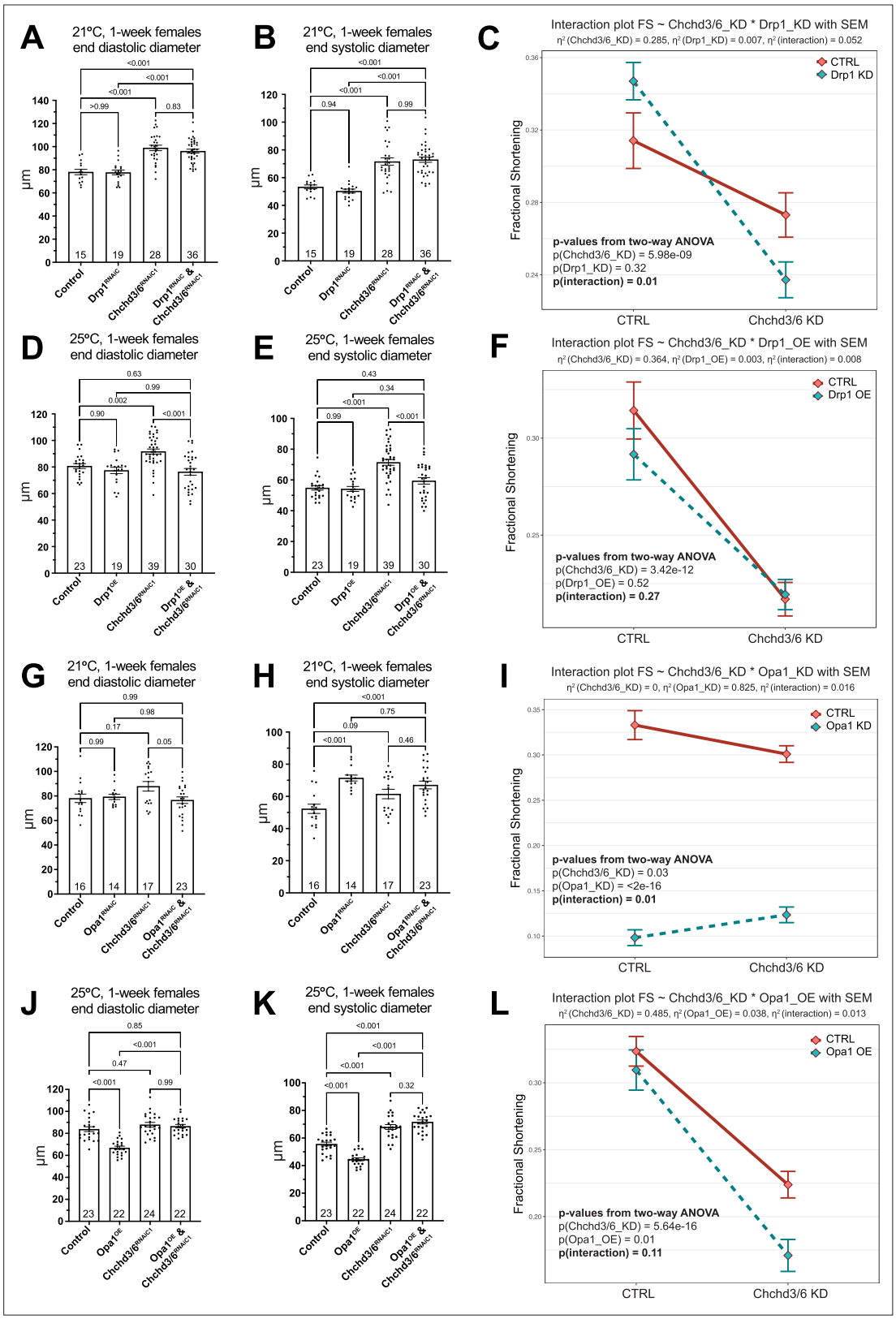

Figure 4—figure supplement 1. Genetic interactions between mitochondrial fission-fusion genes and *Chchd3/6* KD. Diastolic and systolic diameters and Two-way ANOVA interaction plots of fractional shortening. (**A–C**) KD of *Drp1* and *Chchd3/6*, (**D–F**) *Drp1* OE and *Chchd3/6* KD, (**G–I**) *Opa1* KD and *Chchd3/6* KD, and (**J–L**) *Opa1* OE and *Chchd3/6* KD. One-way ANOVA with multiple comparisons shows mean with SEM and detailed p-values. Sample size is shown at bottom of each bar. The two-way ANOVA analyses and interaction plots in (**C**, **F**, **I** and **L**) were obtained in R. η^2 is the effect size used

Figure 4—figure supplement 1 continued on next page

Figure 4—figure supplement 1 continued

in ANOVA, showing the extent that each factor – here including *Chchd3/6*, mitochondrial fission-fusion genes, their interaction and the error - accounts for the variance in the results. Except Opa1 KD, in all the other interaction experiments, *Chchd3/6* was the main effect as shown by larger effect size η^2 than the other factors.

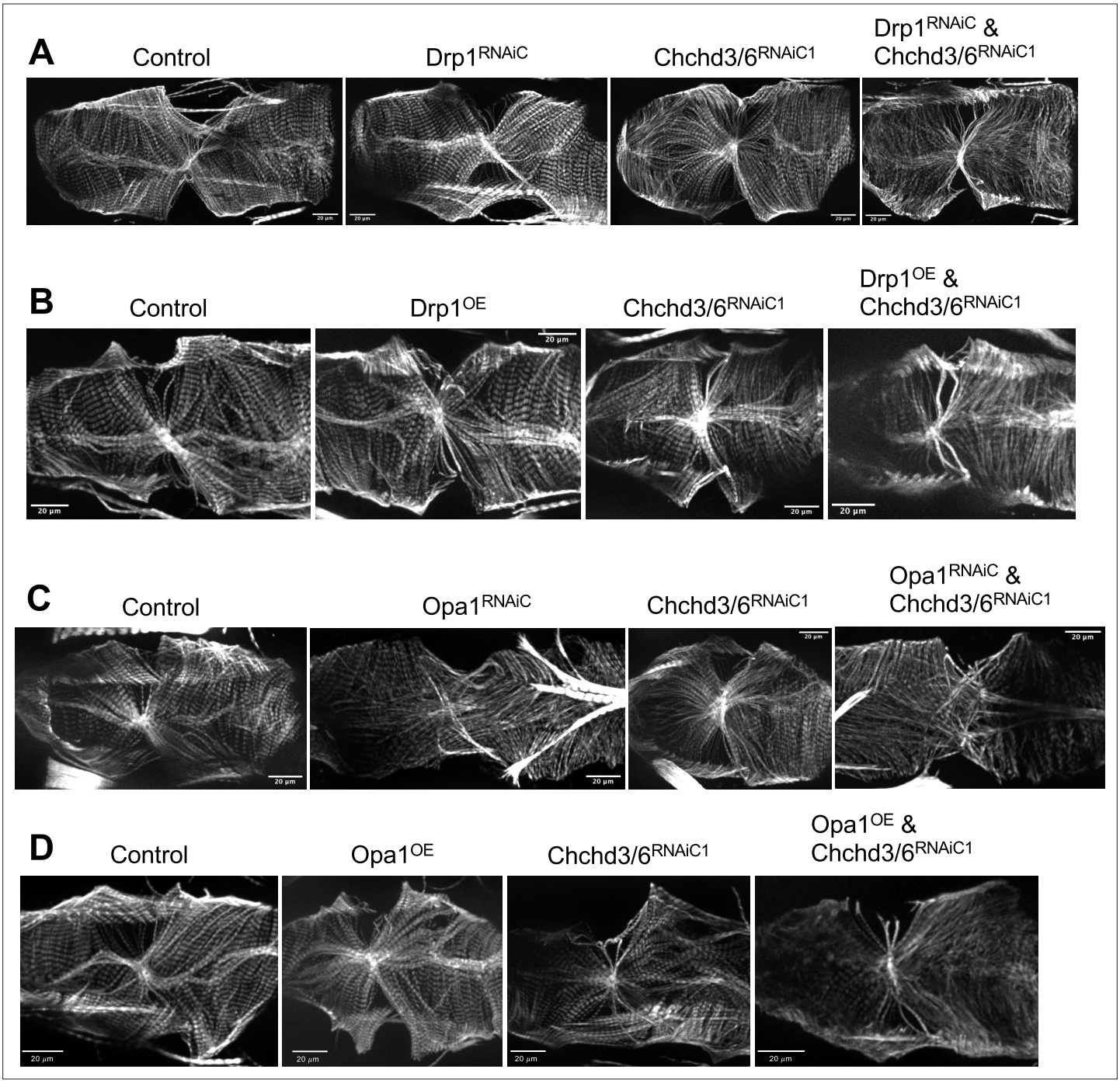

Figure 4—figure supplement 2. F-actin staining of the fly hearts in the interaction experiments involving mitochondrial fission-fusion genes and *Chchd3/6* KD. (**A**) Single and double KD of *Drp1* and *Chchd3/6* at 21 °C. (**B**) Single and double *Drp1* OE and *Chchd3/6* KD at 25 °C. (**C**) Single and double KD of *Opa1* and *Chchd3/6* KD at 21 °C. (**D**) Single and double *Opa1* OE and *Chchd3/6* KD at 25 °C.

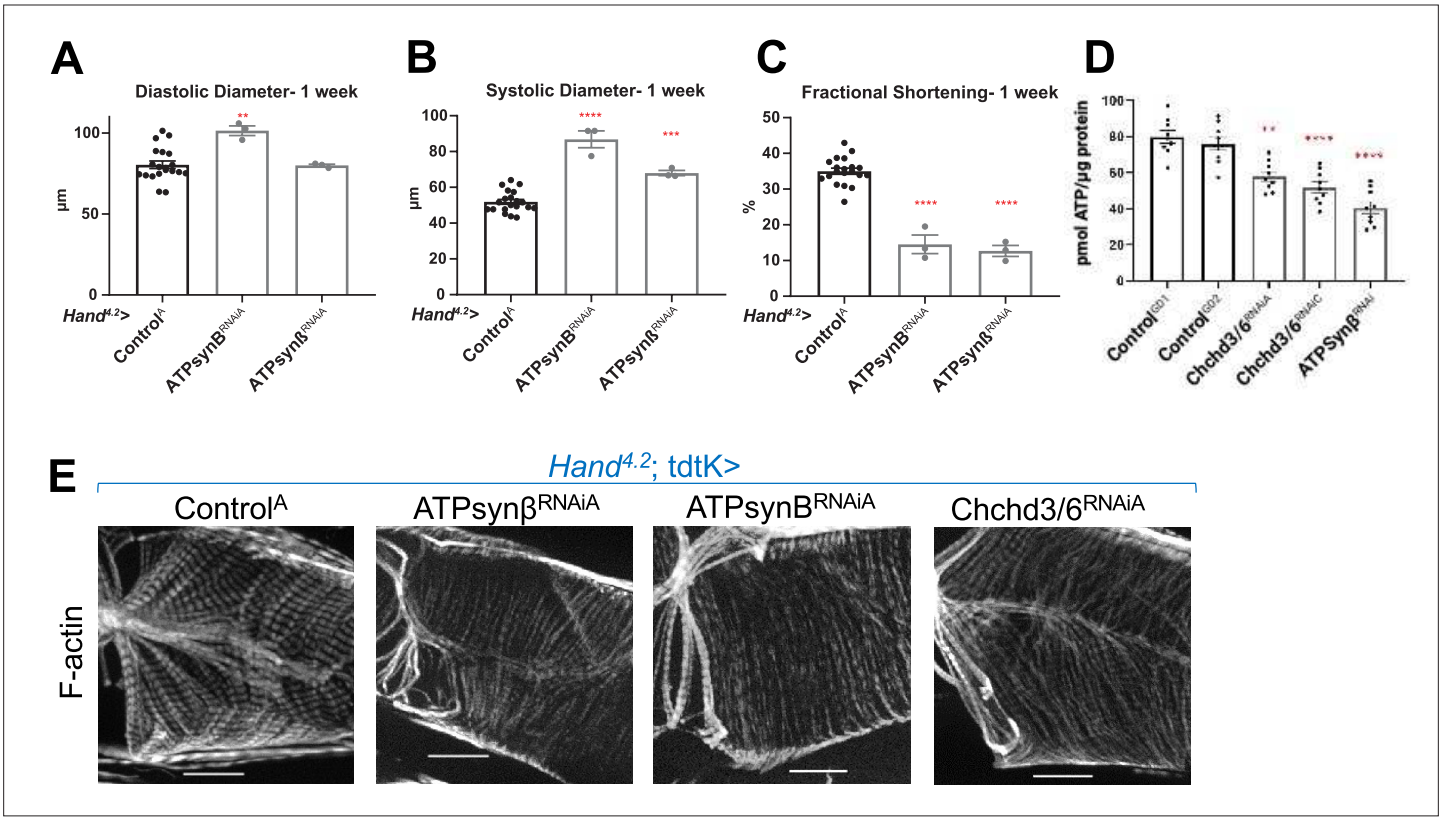

Figure 5. KD of ATP synthase subunit B and beta reduced both fractional shortening and F-actin staining. (**A–C**)*Hand*$^{4.2}$*-Gal4*; tdtK driven KD of ATP synthase subunits at 1 week of age measuring (**A**) diastolic diameter, (**B**) systolic diameter, and (**C**) fractional shortening. Data is plotted as ±SEM and significance indicated relative to Control^{GD2}. ****$P \leq 0.0001$, **$P \leq 0.01$. (**D**) Quantification of ATP levels from hearts of 1 week old flies (10–12 hearts per sample). ATP measurements were plotted relative to protein content. (**E**) 1 week old *Hand*$^{4.2}$*-Gal4*; tdtK driven KD of ATP synthase subunits with altered F-actin (*Chchd3/6* KD is depicted to contrast the structural phenotypes). Statistical differences were calculated by one-way ANOVA followed by Tukey's *post hoc* test for multiple comparisons.

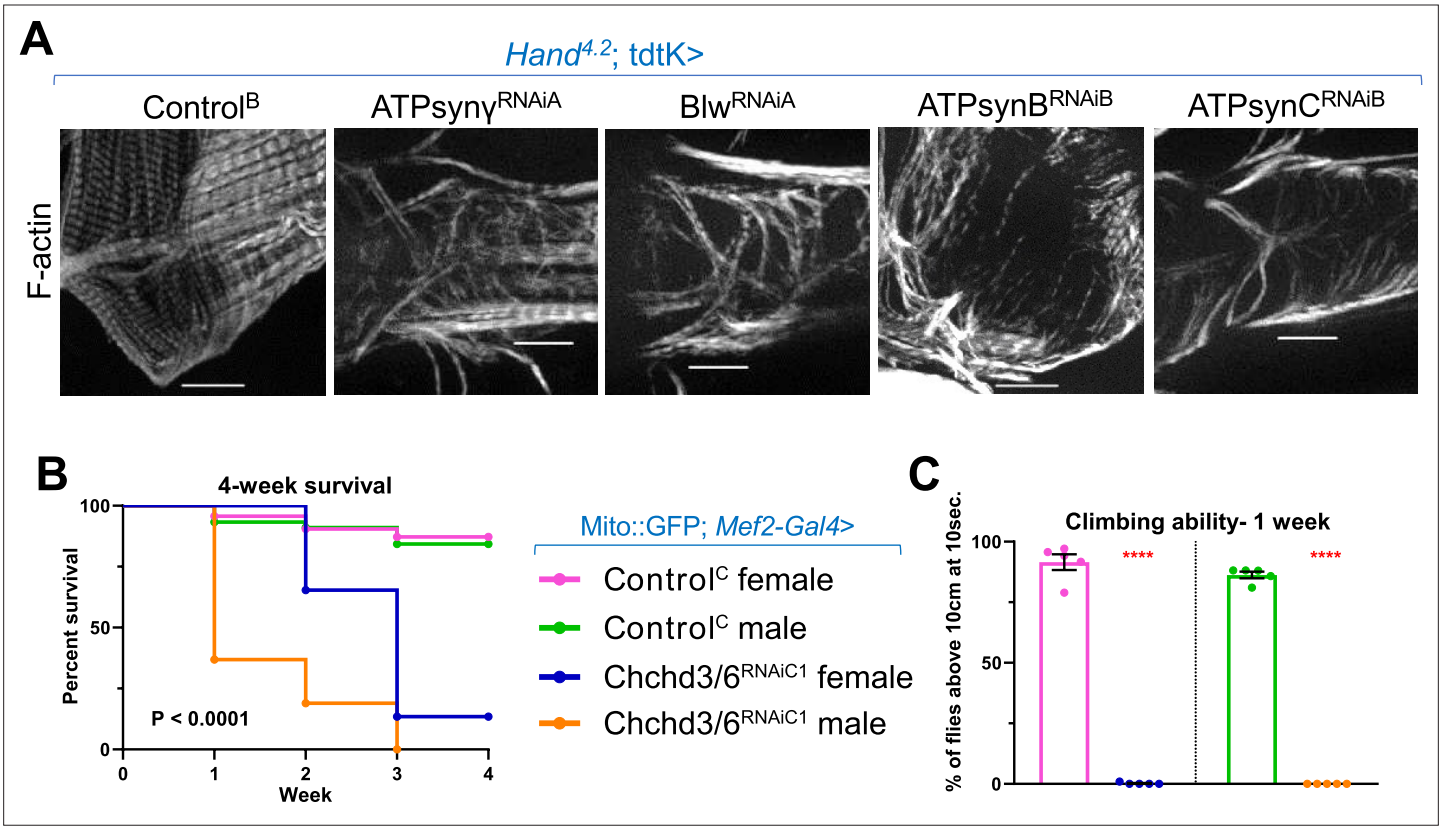

Figure 5—figure supplement 1. (**A**) KD of mitochondrial ATP synthase subunits using *Hand*$^{4.2}$*-Gal4*; tdtK produced strong F-actin phenotypes. 20 µm scale. (**B**&**C**) *Chchd3/6* was knocked down using a Mito::GFP; *Mef2*-Gal4 line; note that Mito::GFP; *Mef2*-Gal4>Chchd3/6^{RNAiA} is pupal lethal. (**B**) Viability was significantly reduced in male and female Chchd3/6^{RNAiC1} flies over a 4 week time course. Mantel-Cox test. (**C**) Negative Geotaxis assay (average number of flies above a 10 cm mark after being tapped down in a long vial) measured in 1 week old male and female flies. Unpaired two-tailed t-test, ****$P \leq 0.0001$; error bars represent SEM.

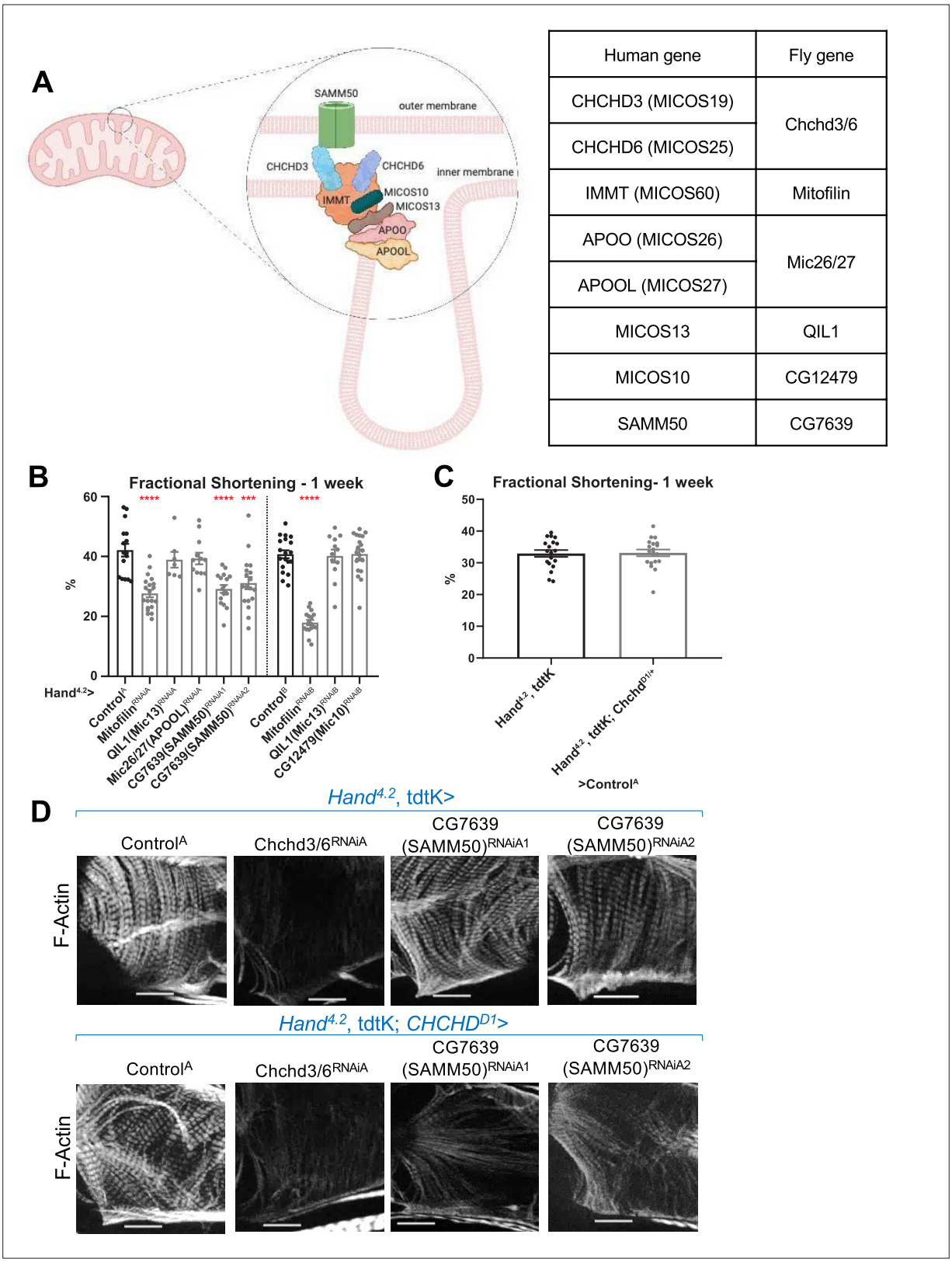

Human gene	Fly gene
CHCHD3 (MICOS19)	Chchd3/6
CHCHD6 (MICOS25)	
IMMT (MICOS60)	Mitofilin
APOO (MICOS26)	Mic26/27
APOOL (MICOS27)	
MICOS13	QIL1
MICOS10	CG12479
SAMM50	CG7639

Figure 6. Assessment of other MICOS subunits in the *Drosophila* heart. (**A**) Schematic of the MICOS complex and SAM50. Human MICOS subunits and their respective *Drosophila* homologs are listed (image created with BioRender.com). (**B**) Fractional shortening measured from 1 week old female flies with KD of individual MICOS subunits and *Sam50* using a *Hand*$^{4.2}$-*Gal4* driver. Unpaired two-tailed t-test, ***$P \leq 0.001$, ****$P \leq 0.0001$; error bars represent SEM. (**C**) *Hand*$^{4.2}$-*Gal4*, tdtK; *Chchd*$^{D1/+}$ line was crossed out with Control^{A}. Unpaired two-tailed t-test, error bars represent SEM. (**D**) 1 week old F-actin-stained *Drosophila* hearts with or without heterozygous loss-of-function *Chchd*$^{D1/+}$ in the background, 20 µm scale.

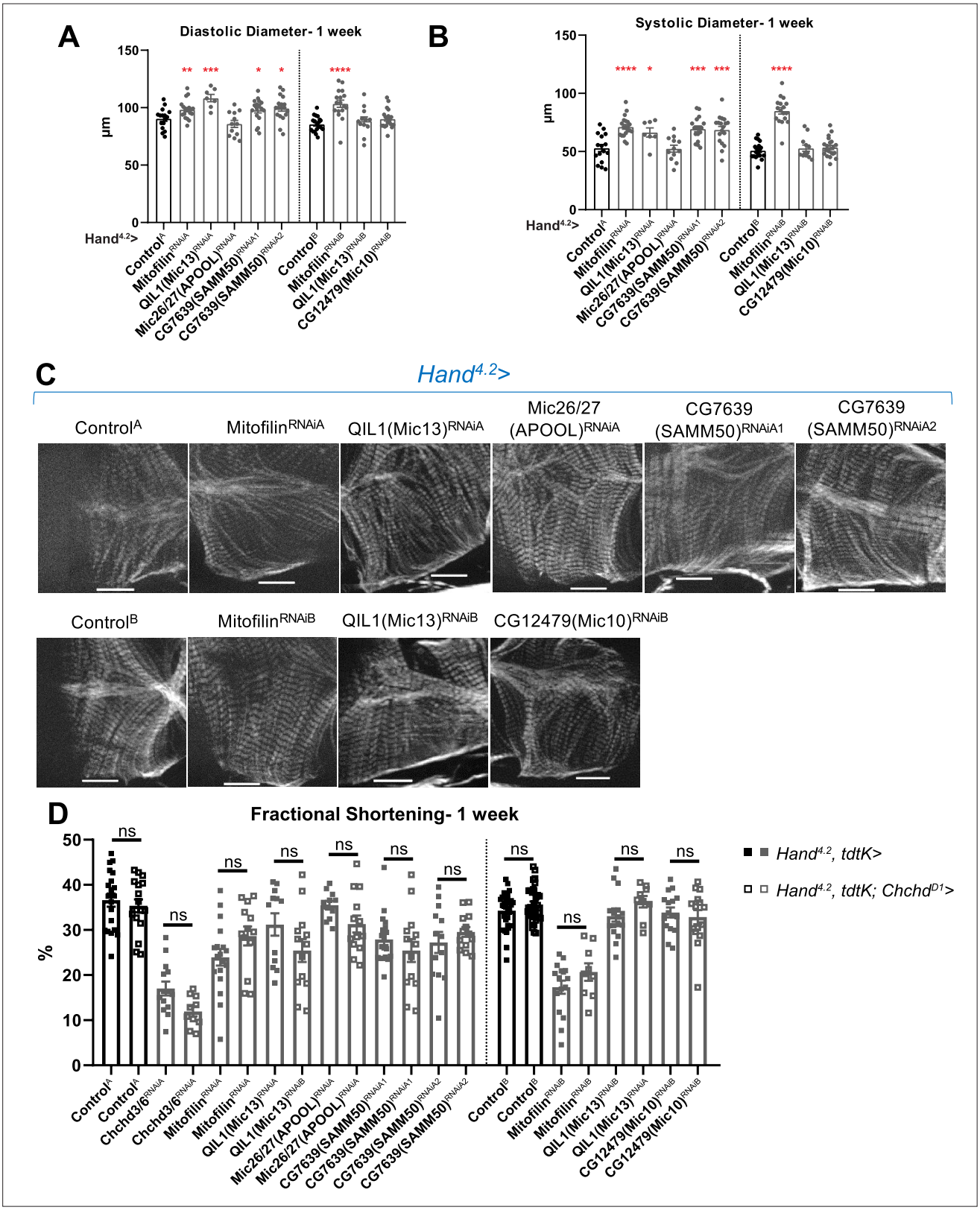

Figure 6—figure supplement 1. (**A**) End-diastolic diameter and (**B**) End-systolic diameter measured from 1 week old female flies with KD of individual MICOS subunits and *CG7639 (SAMM50)* using a *Hand*$^{4.2}$*-Gal4* driver. (**C**) F-actin cardiac sarcomere staining in 1 week old female flies with *Hand*$^{4.2}$*-Gal4* KD. (**D**) All MICOS subunits and *Sam50* were knocked down with *Hand*$^{4.2}$*-Gal4*, tdtK (filled squares) or using the sensitizer line *Hand*$^{4.2}$*-Gal4*, tdtK; *Chchd*$^{D1/+}$ (empty squares) at 25 °C. Two-way ANOVA with Tukey's multiple comparisons test, only statistical comparisons between same RNAi lines are shown; error bars represent SEM, 20 µm scale.

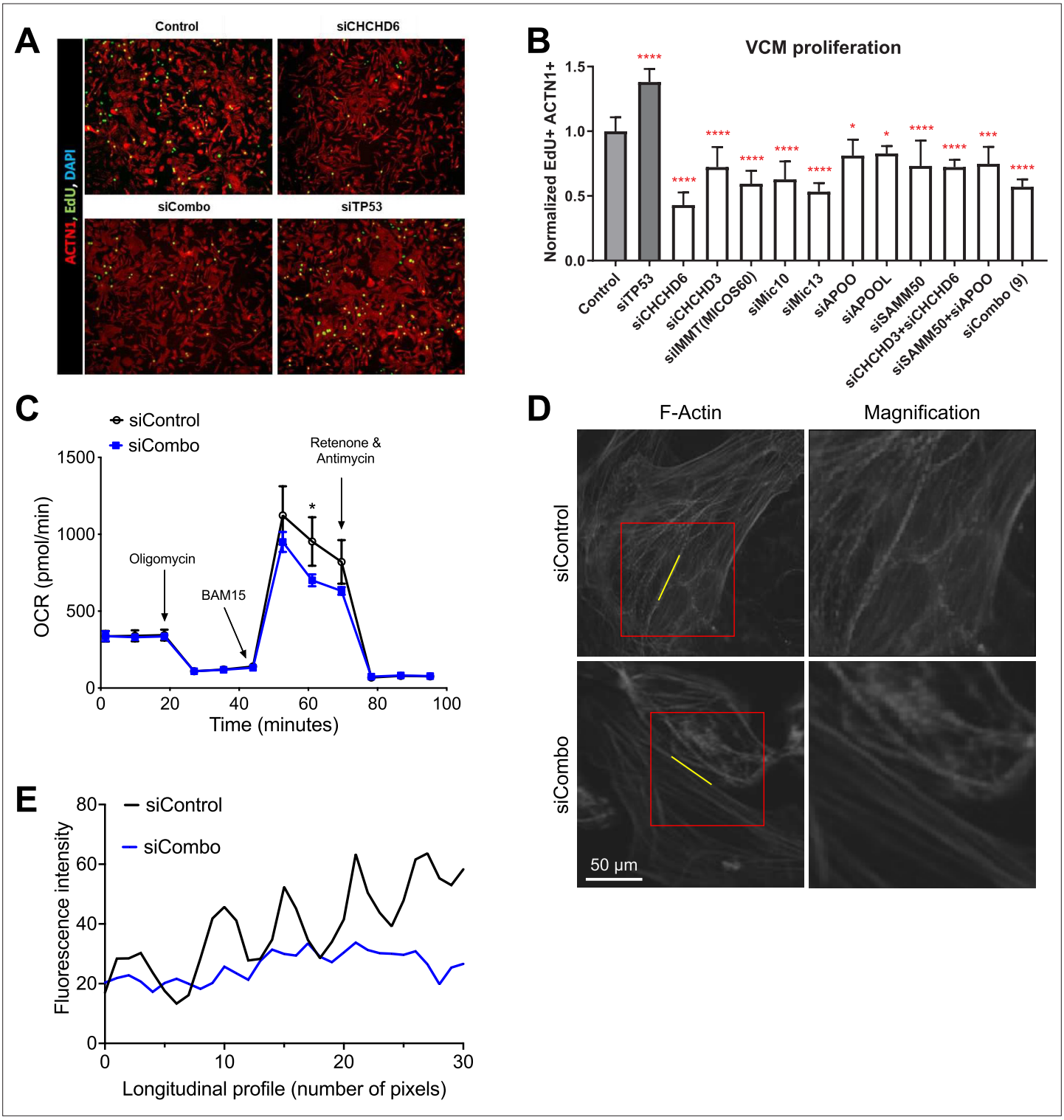

Figure 6—figure supplement 2. Cardiac cell proliferation and contractility assay following MICOS complex subunit KD. (**A**) VCMs showed reduced proliferation with si*CHCHD6*. (**B**) Quantification of proliferation between siRNA mediated KD of individual MICOS subunits and MICOS subunit combination KDs in VCMs (siTP53 is a positive control). One-way ANOVA with Dunnett's multiple comparisons test, *$P \leq 0.05$, ***$P \leq 0.001$, ****$P \leq 0.0001$; error bars represent standard deviation. (**C**) OCR in hiPSC-vCMs after combo KD of *CHCHD3 and CHCHD6* compared to control. (D&E) F-actin staining and fluorescence intensity along the F-actin fiber in combo KD of *CHCHD3 and CHCHD6* compared to control.

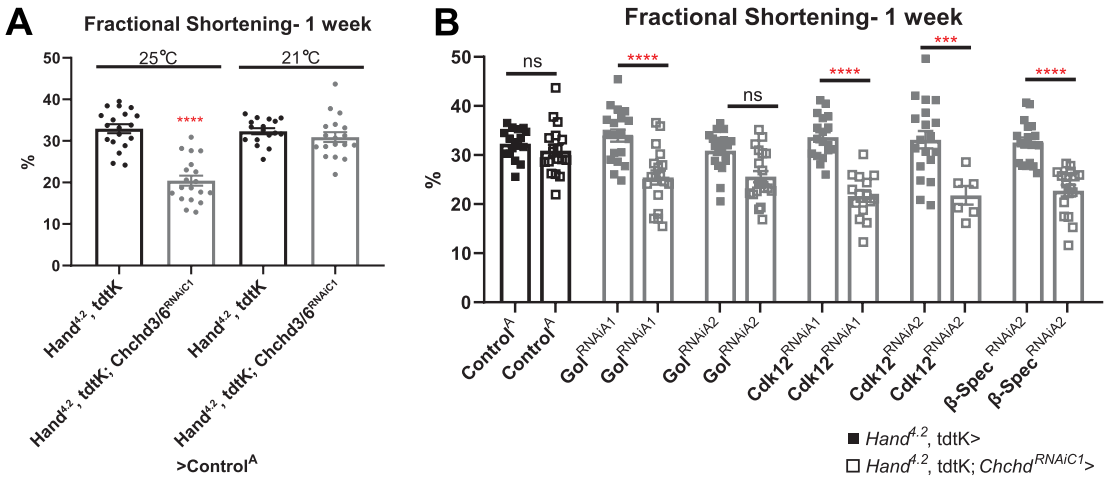

C

					Lethality	
Human gene	**Fly gene**	**DIOPT**	**Function**	**RNAi line**	***Hand4.2*, tdtK>**	***Hand4.2*, tdtK; *Chchd3/6*RNAiC1>**
RNF149	*goliath*	7	Ubiquitination, mesoderm formation	**GolRNAiA1**	0%	0%
				GolRNAiA2	0%	0%
CdK12	*Cdk12*	11	Transcription, RNA splicing	**Cdk12RNAiA1**	47%	77%
				Cdk12RNAiA2	50%	88%
SPTBN1	*β-Spectrin*	15	Crosslinks with actin, scaffolding	**β-SpecRNAiA1**	0%	0%

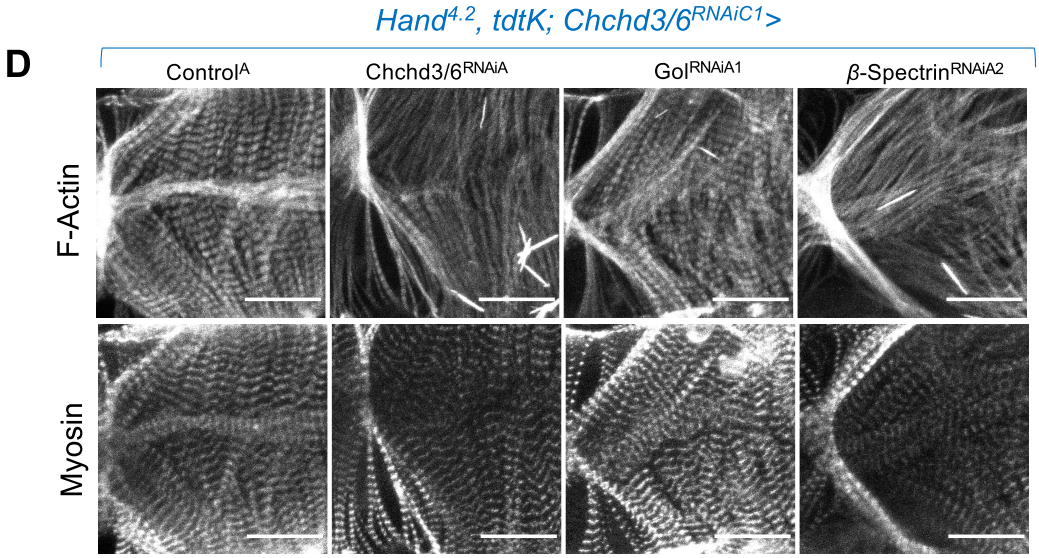

Figure 7. HLHS CHCHD3 and CHCHD6 family-based gene interaction screen reveals three hits. (**A**) A Hand4.2-Gal4, tdtK; Chchd3/6RNAiC1 sensitizer line show reduced fractional shortening at 25°C, which is no longer significant at 21°C. Unpaired two-tailed t-test, ****p≤ 0.0001; error bars represent SEM. (**B**) Genetic interaction of Chchd3/6 and prioritized HLHS candidates. Two-way ANOVA with Tukey's multiple comparisons test, only statistical comparisons between the same RNAi lines are shown; ***p≤ 0.001, ****p≤ 0.0001; error bars represent SEM. (**C**) Functional overview of human and Drosophila orthologs. KD of Ckd12 with Chchd3/6 KD led to increased lethality of eclosed flies by 1 week-of-age.